Degradation of Single-Layer and Few-Layer Graphene by Neutrophil Myeloperoxidase

Rajendra Kurapati,[1] Sourav P. Mukherjee,[2] Cristina Martín,[1,3] George Bepete,[4] Ester Vázquez,[3,5] Alain Pénicaud,[4] Bengt Fadeel,[2] Alberto Bianco[1]*

[1]University of Strasbourg, CNRS, Immunology, Immunopathology and Therapeutic Chemistry, UPR 3572, 67000 Strasbourg, France. E-mail: a.bianco@ibmc-cnrs.unistra.fr

[2]Nanosafety & Nanomedicine Laboratory, Division of Molecular Toxicology, Institute of Environmental Medicine, Karolinska Institutet, Stockholm, Sweden.

[3]Instituto Regional de Investigación Científica Aplicada (IRICA), Universidad de Castilla-La Mancha, Avda Camilo Jose Cela, 13071 Ciudad Real, Spain.

[4]CNRS, Centre de Recherche Paul Pascal (CRPP), UMR 5031, Université Bordeaux, F-33600 Pessac, France.

[5]Departamento de Química Orgánica, Facultad de Ciencias y Tecnologías Químicas, Universidad de Castilla-La Mancha, 13071 Ciudad Real, Spain.

1

Abstract

Biodegradability of graphene is one of the fundamental parameters determining the fate *in vivo* of this material. Here, two types of aqueous dispersible graphene, corresponding to single-layer (SLG) and few-layer graphene (FLG), devoid of either chemical functionalisation or stabilizing surfactants, were subjected to biodegradation by human myeloperoxidase (hMPO) mediated catalysis. Graphene biodegradation was also studied in the presence of activated, degranulating human neutrophils. The degradation of both FLG and SLG sheets was confirmed by Raman spectroscopy and electron microscopy analyses, leading to the conclusion that highly dispersed pristine graphene is not biopersistent.

The biomedical applications of graphene family materials (GFMs) including graphene, graphene oxide (GO), reduced graphene oxide, FLG and graphene nanoribbons are attracting huge attention as ideal components for flexible biomedical electronic devices, implants or for drug delivery.[1] In this context, biodegradation and biocompatibility are two important parameters for translating the use of GFMs in a clinical setting. Earlier studies revealed that the progress in the biomedical applications of GO is limited by some risks of toxicity and mutagenicity.[2] Although biocompatibility can be modulated by covalent or non-covalent functionalisation, biodegradation of GFMs is strongly dependent on oxygen percentage, type of functional groups, defects, lateral size, and number of layers.[3] Biodegradation of GFMs using peroxidases secreted by activated immune cells like neutrophils and eosinophils is one of the major route discovered so far,[4] as demonstrated for oxidised CNTs[4, 5] and GO.[6, 7] Indeed, primary human neutrophils "sense" GO in a size-dependent manner and release so called neutrophil extracellular traps or NETs leading to degradation of the offending material.[6-8] Biomedical applications of GO have been more widely explored,[3] but some recent studies have shown promising results also for graphene. For example, we discovered that FLG dispersions displayed specific killing action on monocytes, showing neither toxic nor activation effects on the other immunocompetent cells. The unique ability of FLG to specifically trigger necrosis of monocytic cells, might be exploited to treat aggressive forms of myelomonocytic leukemia.[9]

Recent results also proved that graphene can be exploited in neural interfaces and flexible devices.[10, 11] However, in the applications as implantable devices or the use as drug delivery system via systemic administration, testing biodegradability or biopersistance of graphene should

be interrogated. Along this line, biodegradation of graphene with oxidative enzymes secreted by cells like neutrophils are very relevant, since this type of cells is the first immune barrier intervening in the case of inflammation. Herein, we study the biodegradation of two types of water dispersible graphene corresponding to FLG and SLG. The biodegradability of these materials was assessed *in vitro* using recombinant human myeloperoxidase (hMPO) and *ex vivo* using freshly isolated neutrophils releasing hMPO extracellularly.

The intrinsic hydrophobicity of the graphene layers prohibits the production of stable graphene aqueous suspension. In the current study, we employed water dispersible FLG and SLG devoid of chemical functionalisation or surfactants to stabilise them in the aqueous media. FLG was produced by mechanochemical exfoliation of graphite thorough interaction with melamine by ball milling treatment in solvent free conditions.[12] After the treatment, water was added to the solid and melamine was removed using dialysis. FLG was stabilised in water or phosphate buffer at 0.1 mg/ml with a final concentration of melamine below 1 ppm (**Figure S1A**).[12] The obtained FLG powder was characterised using TEM, Raman spectroscopy, thermogravimetric and elemental analyses (**Figure S2**). FLG contains around 3.7% of oxygen, corresponding to the presence of few oxygenated groups as also observed by XPS.[12] Raman analysis revealed that the defects are mostly localised at the edges of FLG sheets.[12]

Homogeneously dispersed SLG was instead obtained by oxidising (i.e. electron removal by air exposure) a graphenide (negatively charged graphene, KC_8) solution in tetrahydrofuran, mixing it with degassed water and evaporating the organic solvent to get water dispersed SLG (**Figure S1B**).[13] SLG was characterised using TEM, Raman spectroscopy, XPS and elemental analysis (**Figure S3**). SLG is stable in water by a balance of weak inter-graphene sheet attractive forces and electrostatic repulsion due to spontaneous adsorption of OH^- ions (zeta potential = -45 mV at neutral pH) on the graphene surface obtained from graphenide oxidation.[13] Raman analysis confirmed that SLG is a low-defect graphene due to presence of narrow D and G band linewidths and co-existence of few edge and sp^3 defects due to some functionalisation of the flakes with -H and -OH.[13] The elemental analysis also confirmed that SLG has about 3% of oxygen (**Figure S3D**).

As both FLG (two to four layers) and SLG (monolayer) were obtained using completely different methods, their physicochemical properties are different, likely affecting their behaviour during the degradation process.

The two graphene samples were dispersed in phosphate buffer and treated with hMPO and H_2O_2 for 40 h (see Experimental section in SI). The degradation of both graphene suspensions was carried out adding H_2O_2 every hour and replenishing hMPO every 5 h. The degradation of FLG and SLG was followed by analysing the graphene samples using TEM and Raman spectroscopy at different time-points. First, we employed TEM to visualise the morphological changes of FLG and SLG sheets before and after treatment with hMPO/H_2O_2 (**Figure 1**). After 25 h treatment, flat 2D nanosheets started to become porous, and numerous tiny nanopores were observed on the surface of FLG and their edges were highly crumpled (**Figure 1B**). In addition, some sheets lost their 2D shape (**Figure 1C**). Further significant changes were observed in the morphology of FLG sheets after 40 h, where highly porous residues were formed (**Figure 1D**) along with completely degraded material (**Figure 1E**). A few aggregated sheets were also found confirming the non-uniform degradation due to low-dispersibility of FLG in buffer (**Figure S4A**). We noted that addition of H_2O_2 alone did not affect the morphology of FLG even after 40 h (**Figure 1F**), confirming the strong oxidative nature of the intermediates formed during the enzymatic cycle of hMPO.
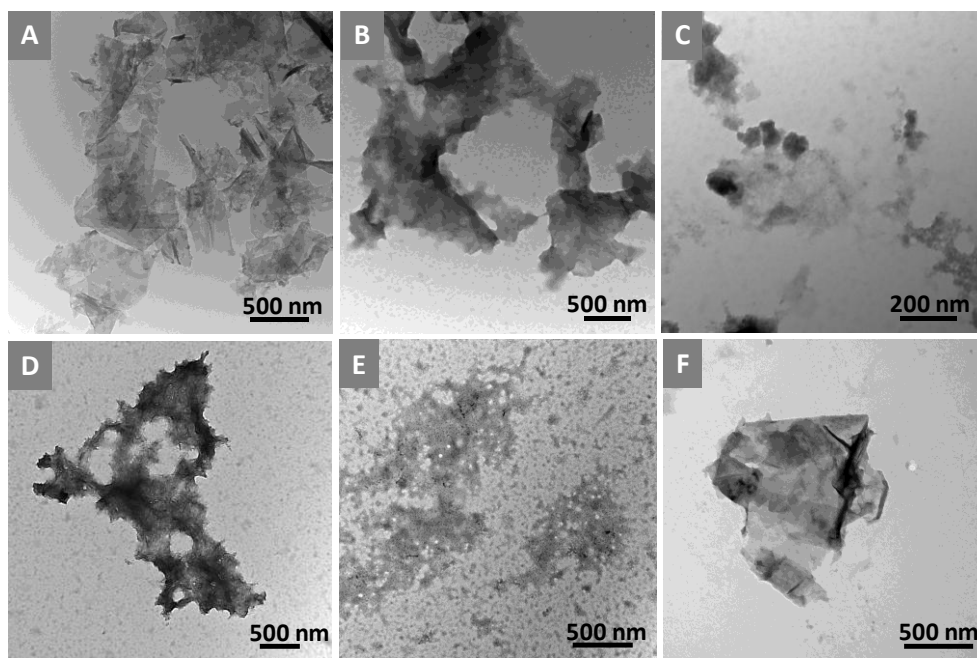
Figure 1: TEM images of FLG. (A) FLG dispersed in phosphate buffer; after treating with hMPO (B-C) for 25 h; (D-E) after 40 h and (F) after treating with H_2O_2 in the absence of hMPO for 40 h.

Similar to the behaviour of FLG, significant differences in morphology were also evidenced for SLG after hMPO treatment (**Figure 2**). Treatment with the enzyme for 25 h drastically affected the structure of SLG (**Figure 2B-C)**. Most of the sheets lost their flat shape leading to highly broken and porous sheets (**Figure 2C**). Prolonging the treatment to 40 h increased further the damages (**Figure 2D-E**), and most of the sheets were broken down to nanoscale fragment. Only a few partially degraded sheets were observed (**Figure S4B**). Importantly, the changes in the morphology of SLG sheets were more drastic compared to FLG after hMPO treatment, which could be explained with a better aqueous dispersibility and the presence of only single-layer graphene sheets in the SLG sample. Control treatment with H_2O_2 alone did not affect the structure of SLG, confirming that the degradation is due to the enzymatic action (**Figure 2F)**.
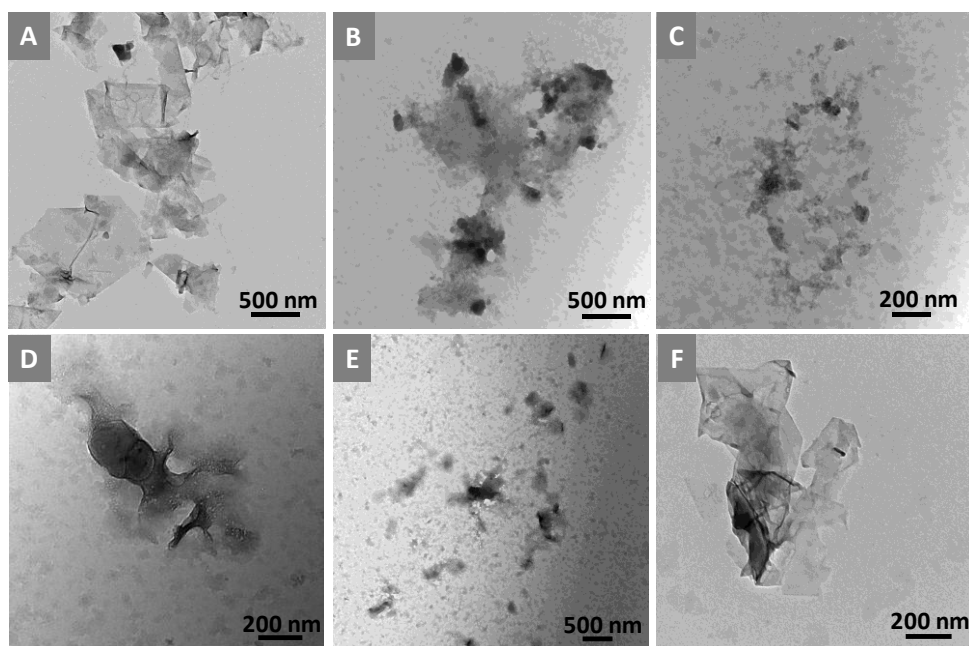
Figure 2: TEM images of SLG sheets: (A) dispersed in phosphate buffer; after treating with hMPO (B-C) for 25 h; (D-E) after 40 h and (F) after treating with H_2O_2 in the absence of hMPO for 40 h.

Next, to complement the electron microscopy results, we employed Raman spectroscopy, which is a powerful tool to understand the changes in the structure, quantify the amount of defects and the oxidation level of graphene sheets.[14] We calculated the intensity ratio of D and G bands that indicates the number of defects on the surface of graphene. Initially, the D/G intensity ratio of

FLG sheets dispersed in PBS was 0.51, which is similar to the value reported in the literature (**Figure 3A**).[12] After incubation with hMPO for 25 h, the variation of this ratio was very small (D/G = 0.46). After 40 h, FLG sheets displayed two types of spectra. A series of averaged spectra presented well defined D and G bands (D/G = 0.41), while a second set of spectra were completely devoid of D bands and nearly missing G bands (**Figure 3A**). The drastic decrease of these two bands is due to significant oxidation/degradation of FLG sheets, as observed by TEM. Raman microspectrometric 2D mapping of FLG sample further confirmed the degradation (**Figure S5**).
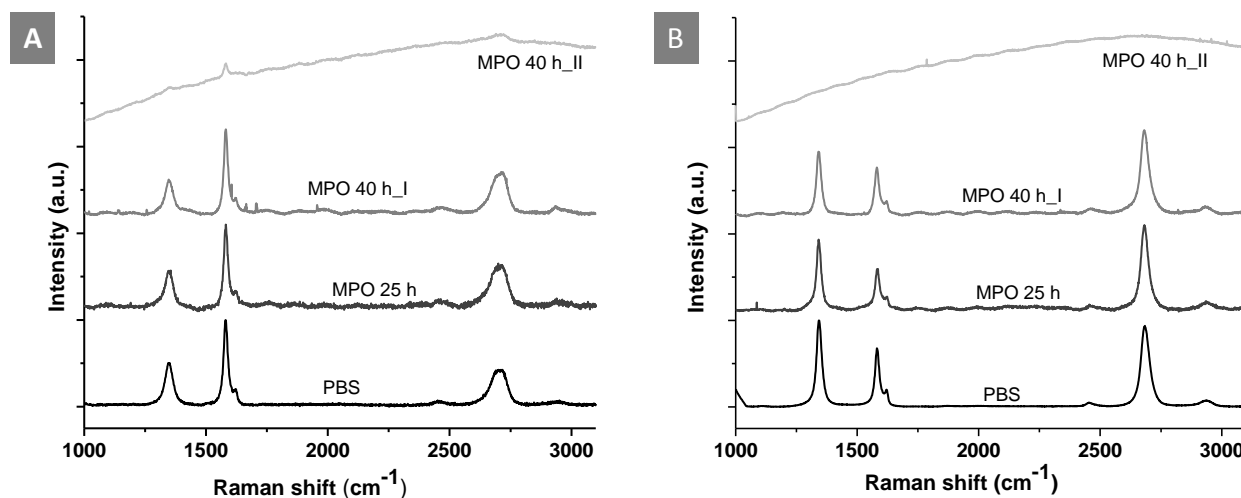
Figure 3: Raman analyses of (A) FLG sheets and (B) SLG sheets before and after treating with hMPO for 25 h and 40 h, respectively.

Raman analyses of SLG sheets also showed a similar trend seen for FLG (**Figure 3B**). SLG sheets dispersed in PBS had a D/G ratio of 1.5.[13, 15] The hMPO treatment for 25 h resulted in an increase of D/G ratio to 1.8, confirming the increase of defects or oxidation of graphene sheets.[16] In addition, the intensities of D and G bands were reduced compared to control samples in PBS. Further, the D/G ratio slightly decreased to 1.42 after 40 h, and the intensities of D and G bands were significantly reduced compared early time points. It should be noted that the sample treated for 40 h showed two types of Raman signatures like FLG (**Figure 3B**). One set of spectra present still defined D and G bands while another series of spectra evidenced the disappearance of D and G bands, explaining the presence of completely degraded graphene sheets as shown by TEM analysis (**Figure 2E**). 2D mapping analysis again supported the degradation of SLG (**Figure S6**). This result also confirms that the degradation of SLG sheets by

hMPO is not completed even after 40 h unlike GO, that is entirely degraded within 24 h.[6, 7] This kind of spectral changes was absent in control samples where FLG and SLG were treated only with H_2O_2 (**Figure S7**).

It is not surprising that graphene is more resistant to enzymatic degradation than GO, as the number of defects and functional groups that are determinant factors for this process are negligible in comparison to those in GO. Overall, the Raman analyses did not support a complete degradation/oxidation of graphene sheets in contrast to the TEM analyses. This could be due to the aggregation of graphene sheets in PBS, which resulted in displaying two kinds of Raman signatures even after 40 h treatment, and the technical limitations of Raman, which does not allow to evidence the presence of the nanoscale and porous fragments. Overall, both Raman and TEM analyses confirmed that some of FLG and SLG sheets were only partially degraded, likely due to low dispersibility or aggregation of graphene sheets into thicker sheets as shown in **Figure S4**. We reported earlier that also aggregated GO sheets could not be degraded by hMPO.[6]

To gain more insights about the interaction between hMPO and graphene samples, we decided to conduct an electrophoresis analysis. As shown in **Figure S8**, SLG displays better interaction with cationic hMPO (arginine rich protein) over FLG because of the high negative surface charge of SLG (zeta potential = -45 mV).[13, 17] Thus, the enhanced interaction between SLG and hMPO could be the driving force for the higher degradability of SLG over FLG sheets (**Figure 2**). We previously noted a similar trend in the hMPO-driven biodegradation of GO samples characterised by different surface charge.[6]

Then, we wanted to assess if hMPO-rich human neutrophils were able to biodegrade FLG and SLG. Our previous works have demonstrated that neutrophils are capable to degrade GO and CNTs extracellularly upon degranulation of oxidative enzymes.[7, 8, 18] The N-formyl-methionyl-leucyl-phenylalanine (fMLP) tripeptide is a potent activator of neutrophils and cytochalasin B (Cyto-B) enhances several fMLP-stimulated neutrophil responses, including aggregation, superoxide production, and degranulation.[19] Freshly isolated primary human neutrophils were activated with fMLP and Cyto-B and incubated with FLG and SLG. Neutrophils activated in this manner were added every day up to five days (**Figure 4A**). Exogenous H_2O_2 was not required, as these neutrophils already contain the complete system required for degradation.[20] The biodegradation of the FLG and SLG was analysed by confocal Raman microspectrometric

7

mapping as shown in **Figure 4B** and **4C**, respectively. FLG was significantly degraded after 5 days, as indicated by the significant reduction of D and G band intensities (**Figure 4B**).
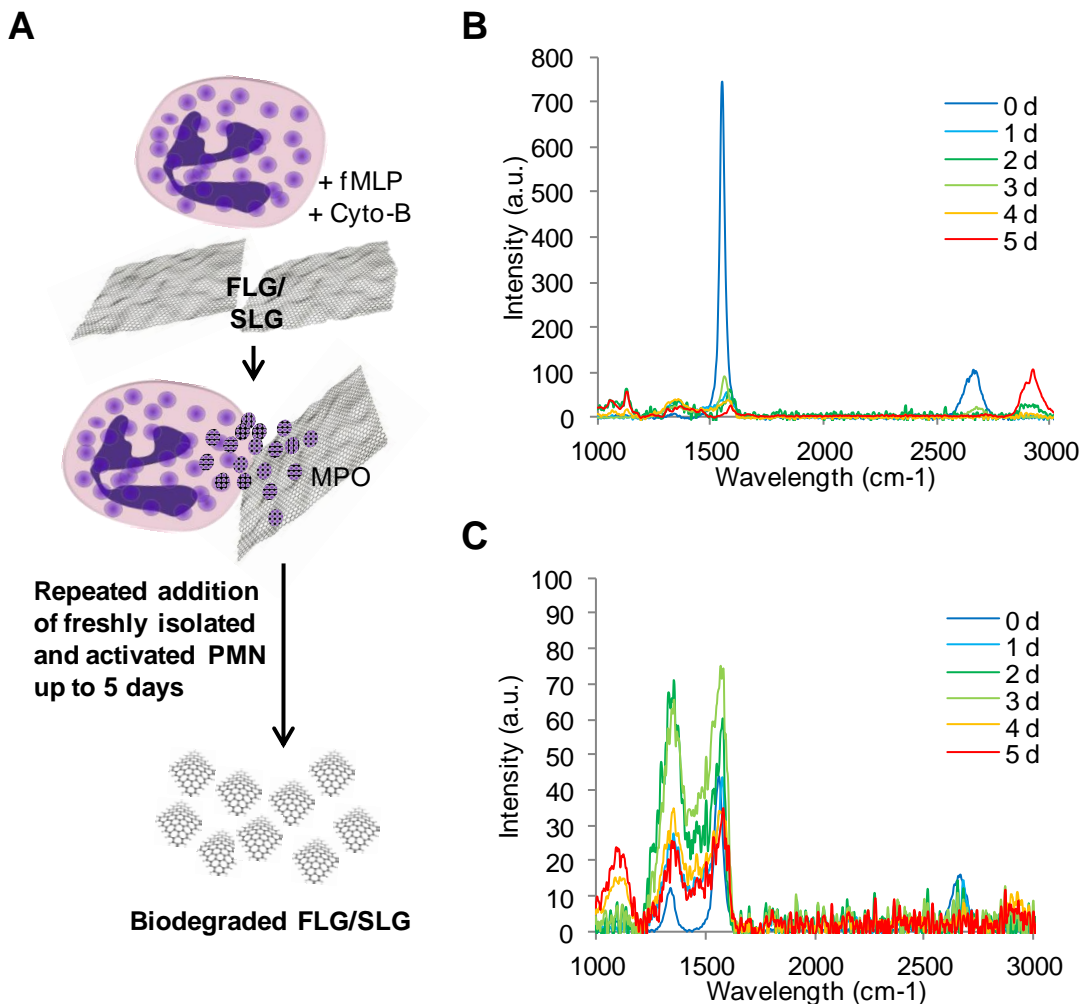

Figure 4. (A) Schematic illustration showing the study design for activated polymorphonuclear leukocyte (PMN)-mediated FLG and SLG degradation. Raman microspectroscopic measurement of FLG (B) and SLG (C) samples following incubation with PMNs.

This was confirmed by Raman 2D mapping analyses of FLG at different time-points, revealing again a remarkable reduction in the G band intensity after 5 days of treatment compared to day 0 (**Figure 5A**). The D/G ratios instead increased along the days of incubation with neutrophils (**Figure 5B** and **5C**) for both FLG and SLG, but at a lower extent for SLG. These D/G increases after 5 days confirmed that oxidation mediated degradation of the graphene sheets has

occurred.[6, 7] In addition, the peak enlargement,[21] leading to the lack of separation between the D and G bands for SLG (**Figure 4C**), together with the disappearance of the characteristic 2D band, further support a reduction of the degree of graphitization and the creation of defects on graphene sheets.
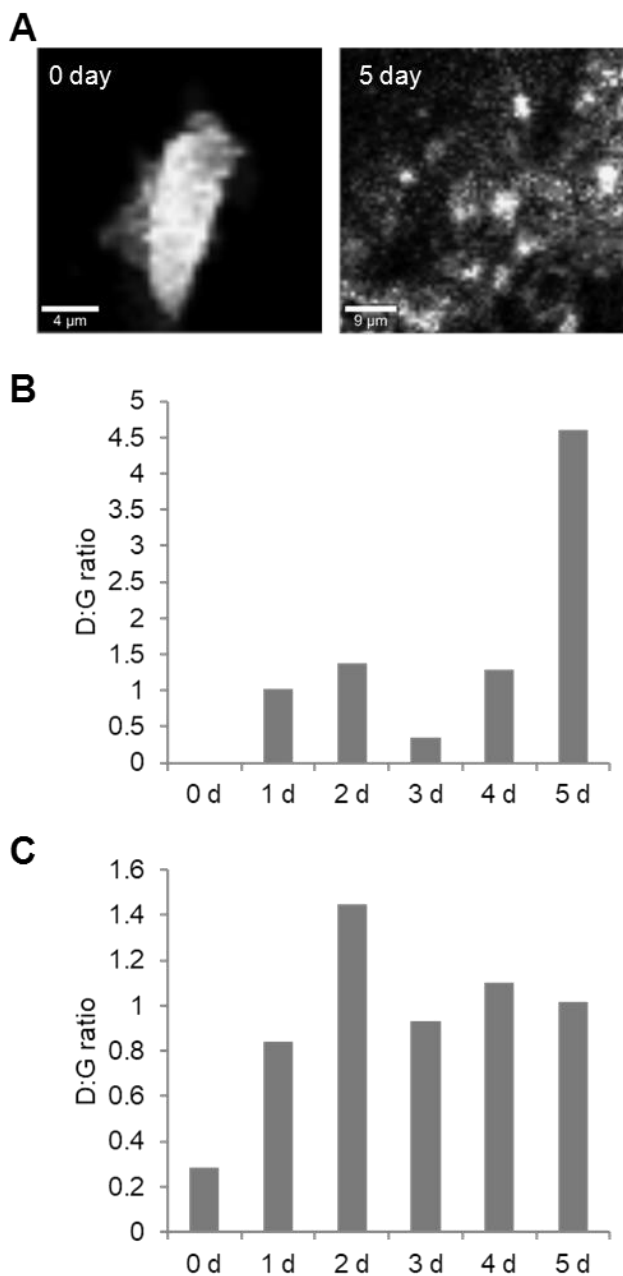
Figure 5. (A) G band images of FLG samples at different time-points showing reduction in the G band intensity (scale bar: 4 and 9 µm). The D/G band ratio of FLG (B) and SLG (C) was increased with PMN incubation time indicating incorporation of greater defects due to degradation of the flakes.

Taken together, these results showed that activated primary human neutrophils can digest both FLG and SLG. SLG sheets were degraded at lower speed compared to FLG sheets by the neutrophils, likely due to the presence of minor number of defects and lower content of oxygenated functions on the surface of SLG sheets compared to FLG sheets. Since FLG was obtained by mechanical ball-milling and subsequent dispersion, whereas SLG sheets were synthesised by direct exfoliation in solution, a high quality graphene sheets is likely present in SLG.[13] In comparison to isolated hMPO, the cellular system deployed here seems to be more efficient in degrading FLG than SLG.

Overall, the treatment of graphene sheets either *in vitro* in the presence of recombinant hMPO or using activated neutrophils, suggested that degradation of pristine graphene sheets is also possible, similarly to degradation of other carbon materials like oxidised CNTs or GO.[4, 6, 7, 18] Though FLG and SLG have only a slightly different oxygen content (~3.7% and 3%, respectively), they have different types of defects and functional groups at their edges. While FLG has some oxygenated groups like epoxides, carbonyl and carboxylates,[12] SLG has defects derived from the modification of the edges by protons and hydroxyls. Overall, comparing the degradation of few-layer graphene to that of single-layer graphene based on their oxygen content remain difficult to rationalise. The degradation is triggered by the generation of reactive intermediates of hMPO in the presence of H_2O_2 and NaCl. In particular, the highly oxidant reactive intermediate hypochlorite (NaOCl, $E^o = 1.56$ V) is the main species able to oxidise and degrade the graphene sheets. In the case of GO, we found that the total degradation process encompasses 24 h.[6, 7] Since graphene does not have oxygenated functional groups and defects like GO, we can expect that it would be more difficult to degrade pristine graphene sheets. Earlier studies dealing with *in vivo* and *in vitro* macrophage degradation of carboxyl functionalised graphene (graphene treated with HNO_3) revealed that the degradation of this type of graphene is possible within cells, though the mechanism of degradation was not proven.[22] In addition, our current study further reinforces the idea that pristine graphene is biodegradable, and shows for the first time that neutrophils are capable of extracellular digestion of graphene. Although the *in vitro* degradation and neutrophil degradation of FLG and SLG have shown some differences, the current results add another important element to the safety assessment of GFMs, with potential implications for their *in vivo* use. Previously, Schinwald *et al.* showed that

pulmonary exposure to pristine graphene nanoplatelets (average lateral dimension: 5 µm, average thickness: ~10 nm) significantly increased the number of neutrophils and eosinophils, 24 h post-exposure compared to the control mice.[23] The acute inflammation reaction in the lungs was reduced after 7 days presumably due to the degradation of graphene platelets into smaller fragments. Notably, the material was too large to be completely phagocytosed by macrophages and it stands to reason that extracellular digestion of these materials may come into play, along with other clearance mechanisms. Our results show that pristine graphene sheets, from single- to few-layers of a few hundred nanometers in lateral size, can be degraded by the action of activated neutrophils, albeit at a slower rate than GO,[7] further supporting the potential of water dispersible graphene for biomedical applications.

To summarise, we have demonstrated that graphene can be degraded either by recombinant hMPO or by hMPO secreted by activated neutrophils. Two different graphene samples, SLG and FLG, showed different degradability behaviour due to their different physicochemical properties, resulting from differences in the synthesis methods. These results clearly demonstrate that pristine graphene with minimum defects can be degraded by hMPO-mediated oxidation, indicating that our immune system has strategies to degrade graphene materials.

References

[1] K. S. Novoselov, V. I. Falko, L. Colombo, P. R. Gellert, M. G. Schwab, K. Kim, *Nature* **2012**, *490*, 192-200.

[2] H. Pieper, S. Chercheja, S. Eigler, C. E. Halbig, M. R. Filipovic, A. Mokhir, *Angew. Chem. Int. Ed.* **2016**, *55*, 405-407.

[3]   G. Reina, J. M. Gonzalez-Dominguez, A. Criado, E. Vazquez, A. Bianco, M. Prato, *Chem. Soc. Rev.* **2017**, *46*, 4400-4416.

[4]   V. Kagan, N. Konduru, W. Feng, B. Allen, J. Conroy, Y. Volkov, I. Vlasova, N. Belikova, N. Yanamala, A. Kapralov, Y. Tyurina, J. Shi, E. Kisin, A. Murray, J. Franks, D. Stolz, P. Gou, J. Klein-Seetharaman, B. Fadeel, A. Star, A. Shvedova, *Nat. Nanotechnol.* **2010**, *5*, 354 - 359.

[5]   J. Russier, C. Ménard-Moyon, E. Venturelli, E. Gravel, G. Marcolongo, M. Meneghetti, E. Doris, A. Bianco, *Nanoscale* **2011**, *3*, 893-896.

[6]   R. Kurapati, J. Russier, M. A. Squillaci, E. Treossi, C. Ménard-Moyon, A. E. Del Rio-Castillo, E. Vázquez, P. Samorì, V. Palermo, A. Bianco, *Small* **2015**, *11*, 3985-3994.

[7]   S. P. Mukherjee, A. R. Gliga, B. Lazzaretto, B. Brandner, M. Fielden, C. Vogt, L. Newman, A. F. Rodrigues, W. Shao, P. M. Fournier, M. S. Toprak, A. Star, K. Kostarelos, K. Bhattacharya, B. Fadeel, *Nanoscale* **2018**, *10*, 1180-1188.

[8]   S. P. Mukherjee, B. Lazzaretto, K. Hultenby, L. Newman, A. F. Rodrigues, N. Lozano, K. Kostarelos, P. Malmberg, B. Fadeel, *Chem* **2018**, *4*, 334-358.

[9]   J. Russier, V. León, M. Orecchioni, E. Hirata, P. Virdis, C. Fozza, F. Sgarrella, G. Cuniberti, M. Prato, E. Vázquez, A. Bianco, L. G. Delogu, *Angew. Chem. Int. Ed.* **2017**, *56*, 3014-3019.

[10]   K. Kostarelos, M. Vincent, C. Hebert, J. A. Garrido, *Adv. Mater.* **2017**, *29*, 1700909.

[11]   N. P. Pampaloni, M. Lottner, M. Giugliano, A. Matruglio, F. D'Amico, M. Prato, J. A. Garrido, L. Ballerini, D. Scaini, *Nat. Nanotechnol.* **2018**, doi: 10.1038/s41565-018-0163-6.

[12]   V. Leon, J. M. Gonzalez-Dominguez, J. L. G. Fierro, M. Prato, E. Vazquez, *Nanoscale* **2016**, *8*, 14548-14555.

[13]   G. Bepete, E. Anglaret, L. Ortolani, V. Morandi, K. Huang, A. Pénicaud, C. Drummond, *Nat. Chem.* **2016**, *9*, 347-352.

[14]   L. G. Cançado, A. Jorio, E. H. M. Ferreira, F. Stavale, C. A. Achete, R. B. Capaz, M. V. O. Moutinho, A. Lombardo, T. S. Kulmala, A. C. Ferrari, *Nano Lett.* **2011**, *11*, 3190-3196.

[15]   G. Bepete, A. Pénicaud, C. Drummond, E. Anglaret, *J. Phys. Chem. C* **2016**, *120*, 28204-28214.

[16]   F. Torrisi, T. Hasan, W. Wu, Z. Sun, A. Lombardo, T. S. Kulmala, G.-W. Hsieh, S. Jung, F. Bonaccorso, P. J. Paul, D. Chu, A. C. Ferrari, *ACS Nano* **2012**, *6*, 2992-3006.

[17]   A. Klinke, C. Nussbaum, L. Kubala, K. Friedrichs, T. K. Rudolph, V. Rudolph, H.-J. Paust, C. Schröder, D. Benten, D. Lau, K. Szocs, P. G. Furtmüller, P. Heeringa, K. Sydow, H.-J. Duchstein, H. Ehmke, U. Schumacher, T. Meinertz, M. Sperandio, S. Baldus, *Blood* **2011**, *117*, 1350-1358.

[18]   C. Farrera, K. Bhattacharya, B. Lazzaretto, F. T. Andón, K. Hultenby, G. P. Kotchey, A. Star, B. Fadeel, *Nanoscale* **2014**, *6*, 6974-6983.

[19]   P. J. Honeycutt, J. E. Niedel, *J. Biol. Chem.* **1986**, *261*, 15900-15905.

[20]   M. B. Hampton, A. J. Kettle, C. C. Winterbourn, *Blood* **1998**, *92*, 3007-3017.

[21]   A. Sadezky, H. Muckenhuber, H. Grothe, R. Niessner, U. Pöschl, *Carbon* **2005**, *43*, 1731-1742.

[22]   C. M. Girish, A. Sasidharan, G. S. Gowd, S. Nair, M. Koyakutty, *Adv. Healthc. Mater.* **2013**, *2*, 1489-1500.

[23]   A. Schinwald, F. A. Murphy, A. Jones, W. MacNee, K. Donaldson, *ACS Nano* **2011**, *6*, 736-746.

Single-layer and few-layer graphene are degraded by neutrophil myeloperoxidase

Rajendra Kurapati,[1] Sourav P. Mukherjee,[2] Cristina Martín,[1,3] George Bepete,[4] Ester Vázquez[3,5] Alain Pénicaud,[4] Bengt Fadeel,[2] Alberto Bianco[1]*

Supporting Information

Materials and Methods

Materials

Human myeloperoxidase (hMPO) was obtained derived from human neutrophils (Athens Research and Technology, USA) with an activity of 180-220 U·mg^{-1}. Diethylenetriamine pentaacetic acid (DTPA), hydrogen peroxide (30% aqueous solution), NaCl, NaH$_2$PO$_4$·2H$_2$O and Na$_2$HPO$_4$·2H$_2$O were purchased from Alfa Aesar and used directly without any further purification.

Degradation of graphene materials by hMPO

The stock solution of exfoliated graphene is a surfactant-free single-layer graphene (SLG) dispersed in water (0.1 mg/mL). 125 μL of SLG solution was added to 325 μL of 50 mM phosphate buffer (140 mM NaCl + 100 μM DTPA, transition metal chelating agent), to this solution 50 μL of 50 μg of hMPO was added. The total volume of reaction mixture was 500 μL. A 2 μL of 50 mM H$_2$O$_2$ was added every hour. The final concentration of H$_2$O$_2$ was 200 μM. hMPO was renewed for every 5 h up to 40 h in total. The reaction mixture was maintained at 37°C throughout experiment. The final concentration of SLG is 25 μg/mL. As pristine graphene sheets were assumed to be more resistant to oxidation compared to GO[1] and carboxylated CNTs,[2] their degradation was carried out up to 40 h in comparison to 24 h previously used for GO.[1]

Similar to the above experiment, 12.5 µg of few-layer graphene (FLG)[3] lyophilized powder was dispersed in 450 µL of 50 mM phosphate buffer (140 mM NaCl + 100 µM DTPA, transition metal chelating agent). To this solution 50 µL of 50 µg of hMPO was added. The total volume of the reaction mixture was 500 µL. Two µL of 50 mM H_2O_2 was added every hour. The final concentration of H_2O_2 was 200 µM. hMPO was renewed for every 5 h up to 40 h. The reaction mixture was maintained at 37°C throughout the experiment. The final concentration of FLG was 25 µg/mL.

The control experiments treating FLG and SLG with H_2O_2 were also carried out in the absence of hMPO. Both graphene suspensions (25 µg/mL) were prepared in 50 mM phosphate buffer (140 mM NaCl + 100 µM DTPA, transition metal chelating agent). The total volume of reaction mixture was 500 µL. 2 µL of 50 mM H_2O_2 was added every hour. The final concentration of hydrogen peroxide was 200 µM.

The aliquots of treated graphene sheets (add volume) were taken for fixed time intervals, at 0 h, 15 h, 24 h and 40 h and all the samples were stored at -15 °C in a dark room before analysis.

Raman analyses

Raman analysis of *in vitro* degraded samples was performed using Raman spectra Renishaw inVia microRaman equipped with 532 nm laser and a Leica microscope. All samples were prepared by drop-casting 10 µL of respective samples on silicon wafer coated with SiO_2 (20 nm, TED Pella) and dried for 24 h at room temperature. All the spectra were recorded with 1% laser power (0.6 mW) using 100× objective lens. The results reported represent the averages of at least five individual spectra.

Raman microspectrometric 2D mapping of *in vitro* degraded samples was also performed using Raman spectra Renishaw inVia microRaman equipped with 532 nm laser and a Leica microscope. All samples were prepared by drop-casting 10 µL of respective samples on silicon wafer coated with SiO_2 (20 nm, TED Pella). The maps were recorded with 1% laser power (0.6 mW) using 100× objective lens. The scan areas were selected according to the different samples in order to avoid, as far as possible, the zones without nanomaterial. One µm was the measure of the distance between the spectra.

Raman analysis of *ex vivo* degraded samples was performed as previously described[4, 5] using a confocal Raman microspectroscopy (WITec alpha300 system, Germany) with a laser of 532 nm wavelength set at an integration time of 0.5 s and 600× magnification. The scan area for each

sample was adjusted to 100×100 μm. For determination of the intensities of the D-band (second order double resonant mode activated by defects, ~1354 cm^{-1}) and G-band (tangential C–C stretching modes, ~1582 cm^{-1}). The Raman spectrum of each sample is an average of 10000 spectra obtained from a scan size of 100 μm×100 μm.

TEM analysis

Six μL of each aliquot were deposited on carbon coated copper grid and dried under the lamp, and washed the grids in the Milli Q water for ~1 hour to remove the salts (from buffer). All the samples were analysed by a Hitachi H7500 microscope (Tokyo, Japan) with an accelerating voltage of 80 kV, equipped with a AMT Hamamatsu camera (Tokyo, Japan).

Gel electrophoresis

The immobilisation of hMPO on the surface of graphene sheets was evaluated by incubating hMPO with FLG and SLG at room temperature. Briefly, FLG and SLG and hMPO were allowed to interact by mixing together. For SLG, 8 μL of SLG (100 μg/mL in milli-Q water) and 5 μL of hMPO (1 μg/μL in phosphate buffer) and 7 μL of phosphate buffer were incubated for 30 minutes. For FLG, 20 μL of FLG (40 μg/mL in milli-Q water) and 5 μL of hMPO (1 μg/μL in phosphate buffer) were incubated for 30 min. At the end of the incubation time, Laemmli buffer 5 μL was added to the mixture and samples (30 μL) were loaded on a SDS-PAGE 4-15% precasted gel (BioRad). Gel electrophoresis was then run under non-reducing conditions to evaluate the stable electrostatic interaction between hMPO and graphene samples using a Mini-PROTEAN II apparatus (BioRad) and applying a 150 V voltage during 40 min. After electrophoresis, gels were stained with Coomassie Blue (overnight at room temperature) and scanning densitometry was performed with a GS-800™ Calibrated Densitometer (BioRad). The densitometry analysis was then performed using the ImageJ 1.48f software. Signal density was normalised to the hMPO density.

Degradation of graphene materials by neutrophils

Neutrophils were isolated from buffy coats of healthy human blood donors (Karolinska University Hospital, Stockholm, Sweden) as previously described.[6] The samples are completely anonymized and for this reason no specific approval is required. Briefly, neutrophils were isolated from healthy donors every day for 5 consecutive days by density gradient centrifugation using Lymphoprep (Axis Shield, Oslo, Norway) followed by gradient sedimentation in a 5% dextran solution and hypotonic lysis of residual erythrocytes. To study degradation, freshly

isolated neutrophils (10^6 cells/mL) were incubated in phenol red-free RPMI-1640 culture medium (Sigma Aldrich) supplemented with 2 mM L-glutamine, 100 U/mL penicillin and 100 mg/mL streptomycin without serum and incubated in 5% CO_2 at 37°C with FLG or SLG at 20 µg/mL concentration in the presence of fMLP (10 nM) and cytochalasin B (5 µg/mL) (Sigma Aldrich) to trigger degranulation.[7] Freshly isolated, *ex vivo* activated neutrophils were added every day. Samples were collected at the indicated time-points and stored at -80 °C for further analysis.
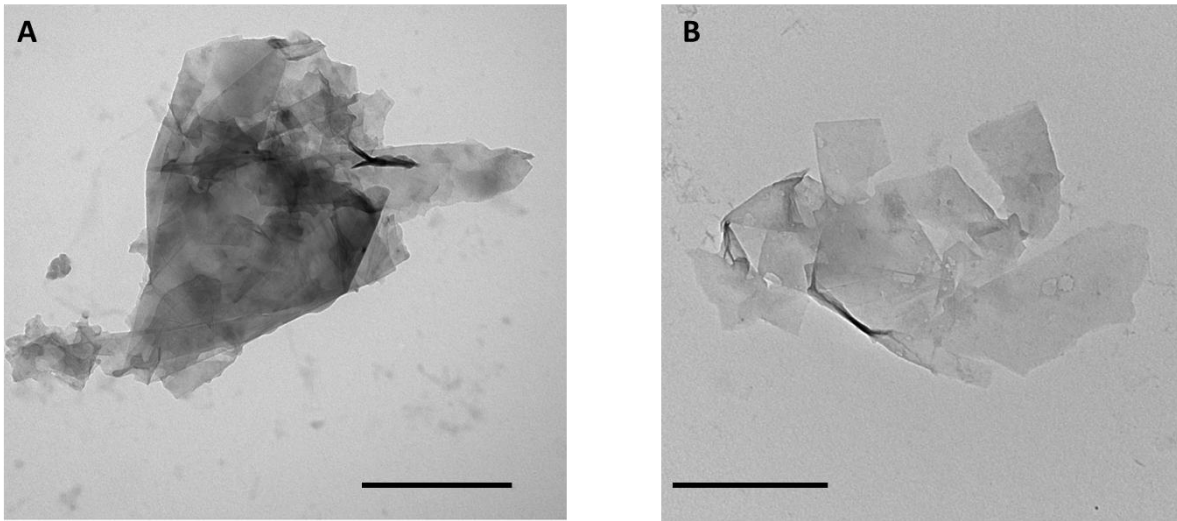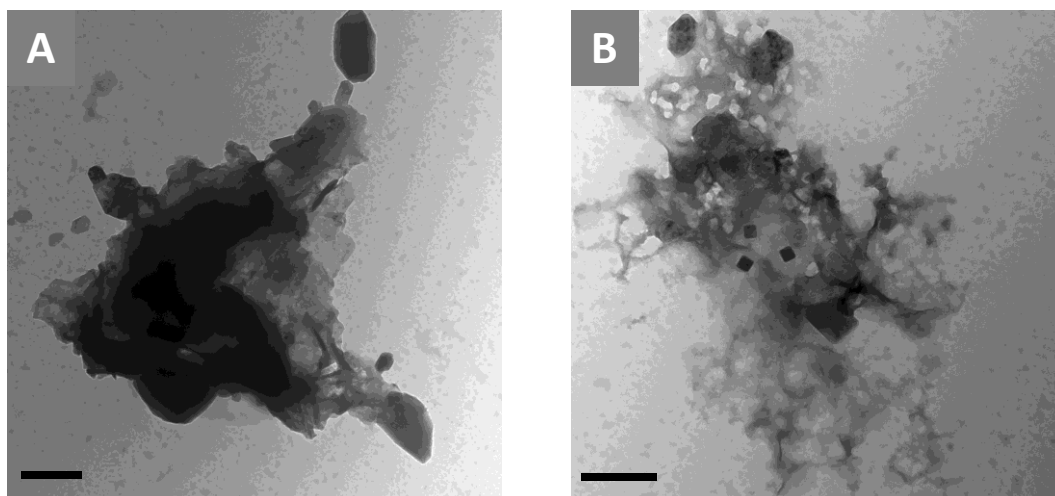

Figure S1: TEM images of (A) FLG and (B) SLG dispersed in phosphate buffer, respectively. Scale bar: 500 nm.
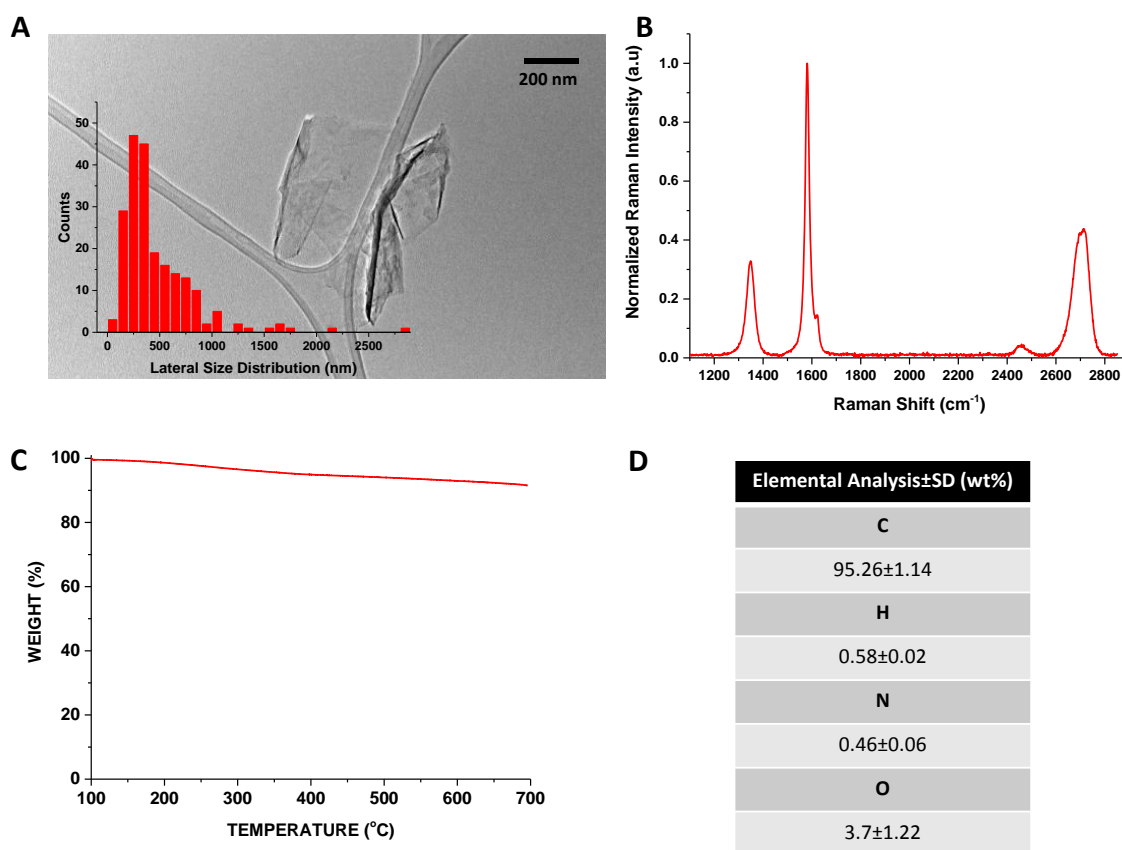
Figure S2: (A) TEM revealed a lateral size distribution of FLG in water dispersion between 200 and 1000 nm, with most of nanosheets around 300 nm. Panel (B) shows Raman average spectrum from FLG, which is composed by the typical graphene Raman bands: G peak, D peak and 2D band, which are centered at ~ 1580 cm^{-1}, ~ 1350 cm^{-1} and ~ 2680 cm^{-1}, respectively. ID/IG = 0.35, and the full-width at half maximum (FWHM) of 2D band is 64.15 cm^{-1}, confirming the few-layer nature of the graphene sample.[3] In addition, the thermal profile for FLG (C) is in agreement with a low content of functional groups, revealing a weight loss of only 6.2% at 600 ºC. Panel (D) displays the elemental analysis of FLG, from which it can be concluded that the sample is mostly composed of carbon. A residual melamine content of 0.69 wt% can be estimated from the atomic content of nitrogen in FLG.

A

B

C

D

Elemental Analysis±SD (wt%)
C
97±1
O
3±1
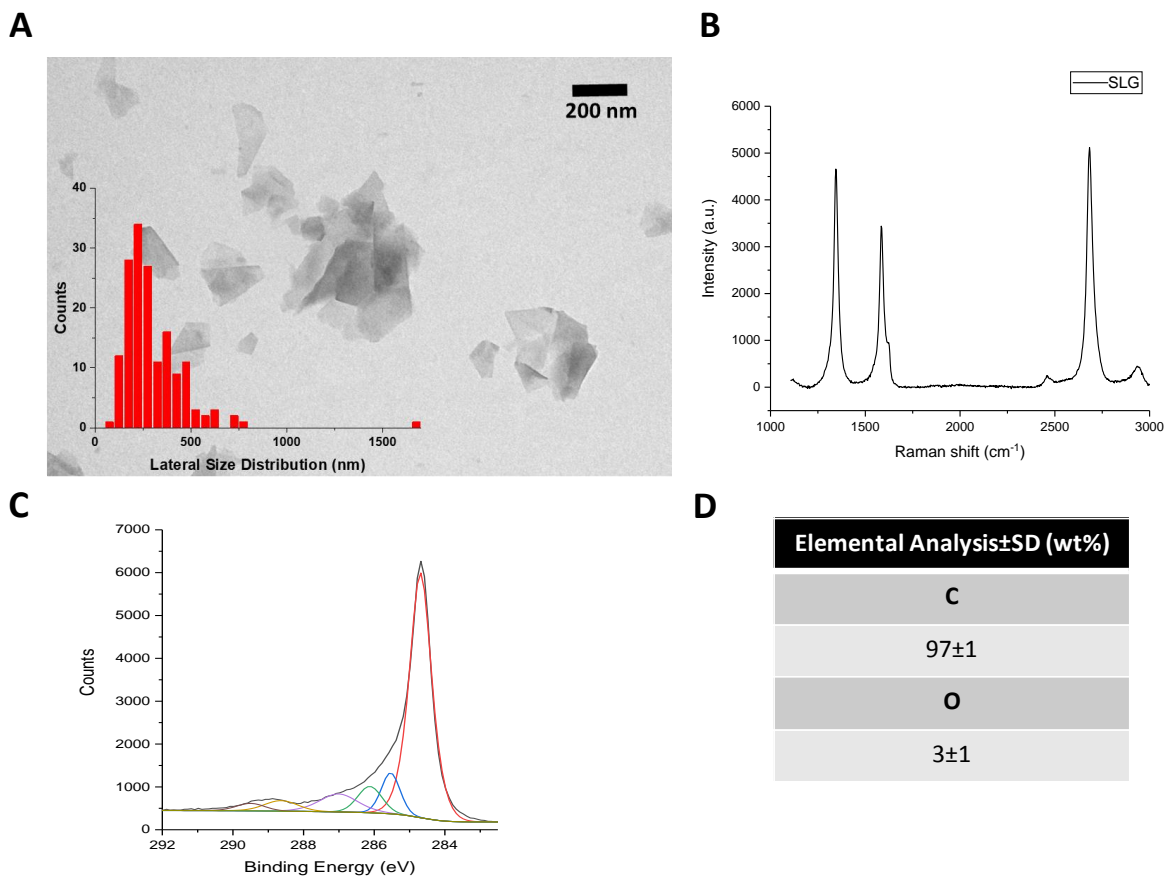
Figure S3: (A) TEM revealed a lateral size distribution of SLG in water dispersion between 200 and 1000 nm, with most of nanosheets around 300 nm. Panel (B) shows Raman spectrum (recorded at 532 nm) of graphene deposits prepared by drop-casting SLG in water on silicon oxide substrate (average of 10 spectra). Raman spectrum is composed by the typical graphene Raman bands: D band, G band, D' band and 2D band, which are centered at ~1345 cm^{-1}, ~1586 cm^{-1}, ~1620 cm^{-1}, and ~2681 cm^{-1}, respectively. ID/IG = 1.50, and the full-width at half maximum (FWHM) of 2D band is 28 cm^{-1}, confirming the single-layer nature of the graphene sample.[8] (C) XPS profile of SLG as deposited film, without any annealing. The C1s X-ray photoelectron spectroscopy analysis of the SLG films shows minor widening on the high-energy side of the C1s peak confirming that there is only little functionalization of the graphene carbon sheets. Panel (D) displays the elemental analysis of SLG, calculated from the fitting of the XPS C1S peak, from which it can be concluded that the sample is mostly composed of carbon.

**Figure S4:** TEM images of (A) FLG and (B) SLG after treating with hMPO for 40 h. Scale bar: 500 nm.
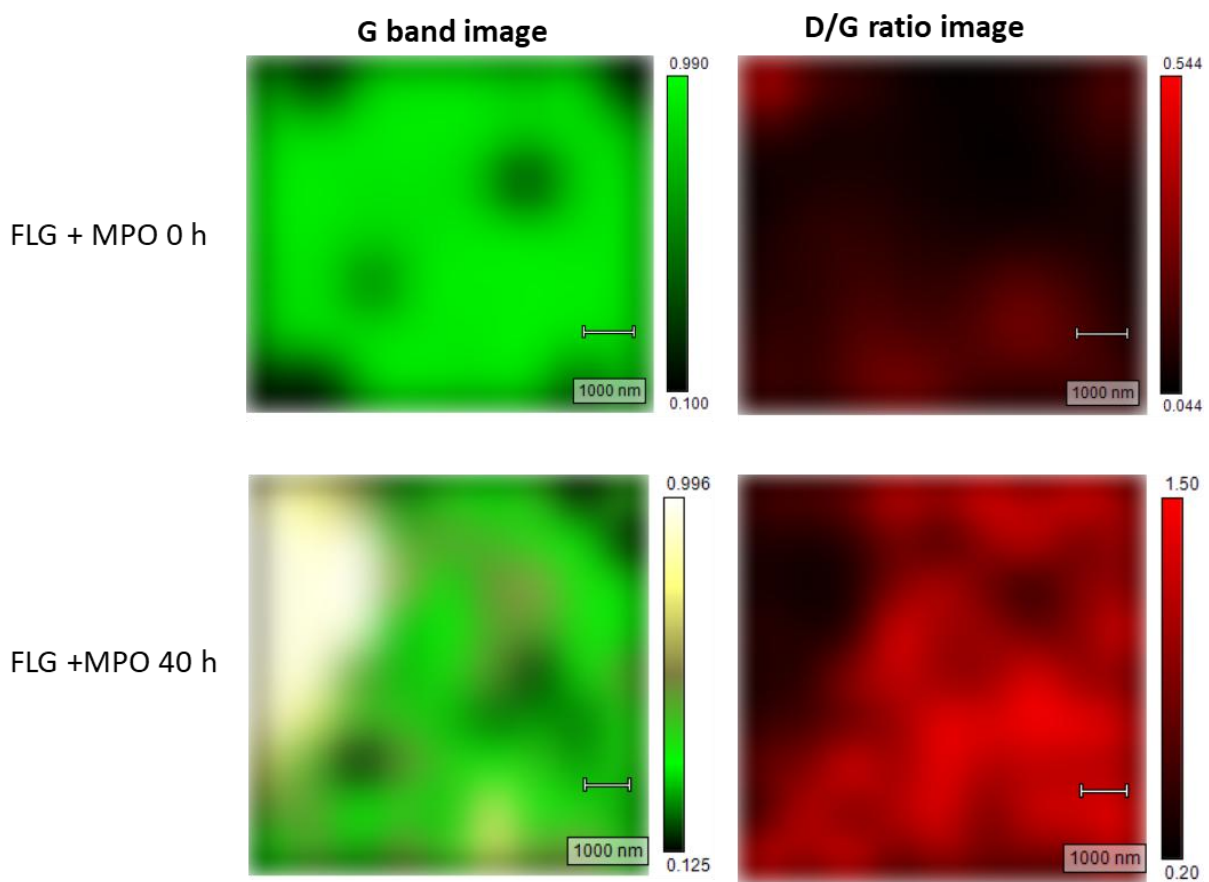
Figure S5. Raman microspectrometric 2D mapping analysis of FLG samples at 0 h (top) and after treating with MPO for 40 h, where G band map images (left side) and D/G ratio map (right

side) are shown. After treating with MPO for 40 h (bottom), we can observe a reduction in the G band intensity, which indicates degradation of the FLG sheets. D/G ratio is also increased compared to 0 h FLG sheets.
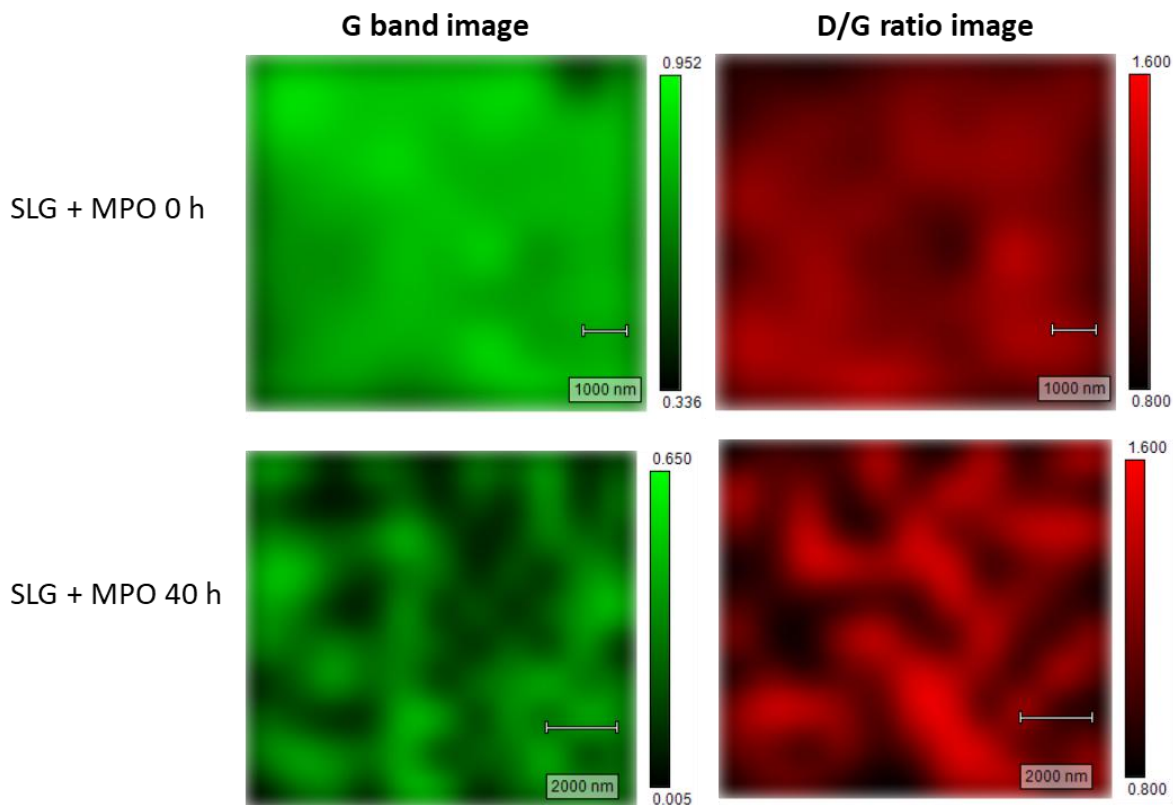
Figure S6. Raman microspectrometric 2D mapping analysis of SLG samples at 0 h (top) and after treating with MPO for 40 h, where G band map images (left side) and D/G ratio map (right side) are shown. After treating with MPO for 40 h (bottom), we can observe a reduction in the G band intensity, which indicates degradation of the SLG sheets. D/G ratio is also increased compared to 0 h SLG sheets.
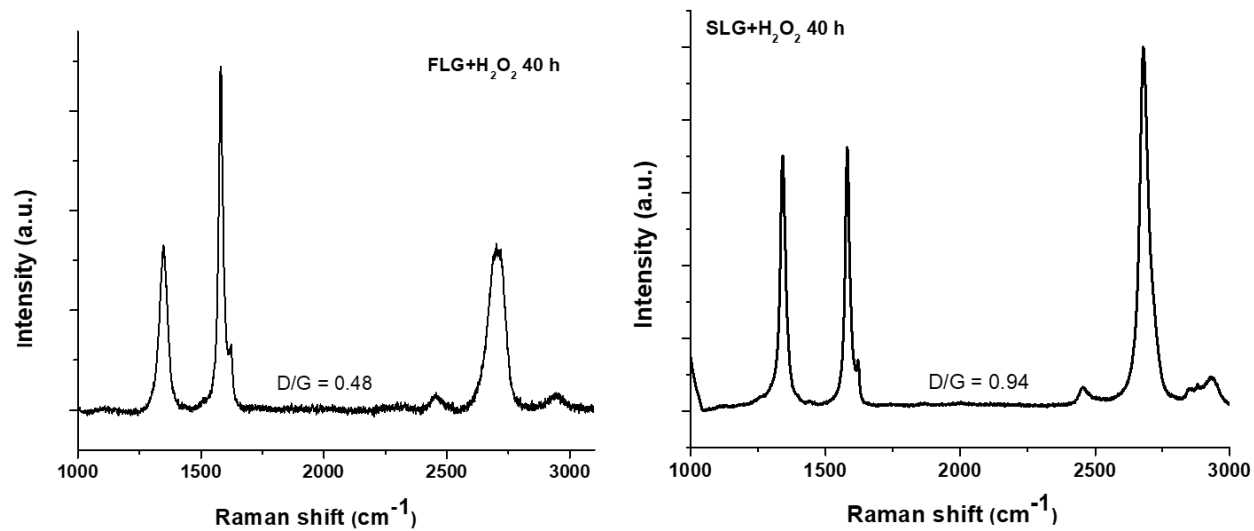
Figure S7: Raman spectra of FLG and SLG sheets, respectively, treated for 40 h with H_2O_2.
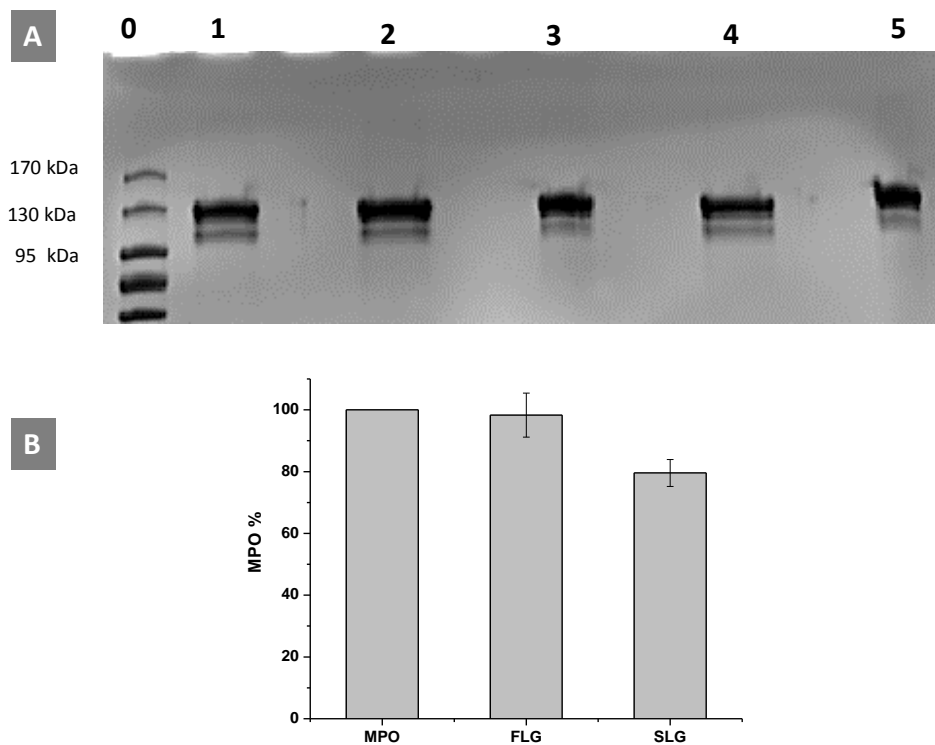
Figure S8: (A) Gel electrophoresis of MPO alone or MPO incubated with FLG and SLG samples. **Lane 0:** Protein ladder; **Lane 1:** hMPO alone; **Lane 2 & 4:** FLG incubated with hMPO; **Lane 3 & 5:** SLG incubated with hMPO. (B) Relative densitometry analysis of the hMPO band (146 kDa): the results are expressed relative to the band of hMPO alone which is considered as 100 % of intensity.

References

[1] R. Kurapati, J. Russier, M. A. Squillaci, E. Treossi, C. Ménard-Moyon, A. E. Del Rio-Castillo, E. Vázquez, P. Samorì, V. Palermo, A. Bianco, *Small* **2015**, *11*, 3985-3994.

[2] V. Kagan, N. Konduru, W. Feng, B. Allen, J. Conroy, Y. Volkov, I. Vlasova, N. Belikova, N. Yanamala, A. Kapralov, Y. Tyurina, J. Shi, E. Kisin, A. Murray, J. Franks, D. Stolz, P. Gou, J. Klein-Seetharaman, B. Fadeel, A. Star, A. Shvedova, *Nat. Nanotechnol.* **2010**, *5*, 354-359.

[3] V. Leon, J. M. Gonzalez-Dominguez, J. L. G. Fierro, M. Prato, E. Vázquez, *Nanoscale* **2016**, *8*, 14548-14555.

[4] F. T. Andõn, A. A. Kapralov, N. Yanamala, W. Feng, A. Baygan, B. J. Chambers, K. Hultenby, F. Ye, M. S. Toprak, B. D. Brandner, A. Fornara, J. Klein-Seetharaman, G. P. Kotchey, A. Star, A. A. Shvedova, B. Fadeel, V. E. Kagan, *Small* **2013**, *9*, 2721-2729.

[5] S. P. Mukherjee, A. R. Gliga, B. Lazzaretto, B. Brandner, M. Fielden, C. Vogt, L. Newman, A. F. Rodrigues, W. Shao, P. M. Fournier, M. S. Toprak, A. Star, K. Kostarelos, K. Bhattacharya, B. Fadeel, *Nanoscale* **2018**, *10*, 1180-1188.

[6] B. Fadeel, A. Åhlin, J.-I. Henter, S. Orrenius, M. B. Hampton, *Blood* **1998**, *92*, 4808.

[7] K. Bhattacharya, C. Sacchetti, R. El-Sayed, A. Fornara, G. P. Kotchey, J. A. Gaugler, A. Star, M. Bottini, B. Fadeel, *Nanoscale* **2014**, *6*, 14686-14690.

[8] G. Bepete, A. Pénicaud, C. Drummond, E. Anglaret, *J. Phys. Chem. C* **2016**, *120*, 28204-28214.